Journal of Solid State Chemistry **155,** 189–197 (2000)
doi:10.1006/jssc.2000.8933, available online at http://www.idealibrary.com on IDEAL®

$La_7Ru_3O_{18}$ and $La_{4.87}Ru_2O_{12}$: Geometric Frustration in Two Closely Related Structures with Isolated RuO_6 Octahedra

P. Khalifah,*,†,[1] Q. Huang,‡,§ D. M. Ho,* H. W. Zandbergen,¶ and R. J. Cava*,†

*Department of Chemistry, Princeton University, Princeton, New Jersey 08544; †Princeton Materials Institute, Princeton University, Princeton, New Jersey 08540; ‡NIST Center for Neutron Research, National Institute of Standards and Technology, Gaithersburg, Maryland 20899; §Department of Materials and Nuclear Engineering, University of Maryland, College Park, Maryland 20742; and ¶National Center for High Resolution Electron Microscopy, Technical University of Delft, Rotterdamsweg 137, 2628AL Delft, The Netherlands

Received June 6, 2000; in revised form August 14, 2000; accepted August 15, 2000

DEDICATED TO PROFESSOR J. M. HONIG

The crystal structures of $La_7Ru_3O_{18}$ and $La_{4.87}Ru_2O_{12}$ have been solved from powder neutron diffraction data ($R_p = 0.032$) and single-crystal X-ray diffraction data ($R_w = 0.070$ for all 3125 reflections), respectively. Although these compounds are both the first example of their structure types, $La_7Ru_3O_{18}$, $La_{4.87}Ru_2O_{12}$, and the known compound $Sr_5Re_2O_{12}$ all have closely related structures. $La_7Ru_3O_{18}$ crystallizes in the rhombohedral space group $R\bar{3}c$, with cell constants of $a = 9.83677(23)$ Å and $c = 56.3493(16)$ Å in the hexagonal setting, and with $Z = 12$ formula units per cell. Monoclinic $La_{4.87}Ru_2O_{12}$ crystallizes in the $P2_1/c$ space group with cell constants of $a = 5.5798(6)$ Å, $b = 10.1286(11)$ Å, $c = 19.0095(20)$ Å, $\beta = 90.815(4)^\circ$, and $Z = 4$. These structures contain isolated RuO_6 octahedra ($d_{Ru-Ru} \sim 5.7$ Å), which are organized into well-defined layers having trigonal or pseudo-trigonal symmetry. Furthermore, the three-dimensional patterning of Ru atoms is a nearly perfect close-packed arrangement, despite the large Ru–Ru distances. Magnetic measurements show that geometric frustration suppresses the ordering of the Ru spins and that monoclinic $La_{4.87}Ru_2O_{12}$ is more frustrated than rhombohedral $La_7Ru_3O_{18}$.

Key Words: **geometric frustration; antiferromagnets; lanthanum ruthenium oxides; valence bond sum; $La_7Ru_3O_{18}$; $La_{4.87}Ru_2O_{12}$; $Sr_5Re_2O_{12}$.**

INTRODUCTION

Most investigations on the properties of ruthenium oxides have focused on well-known structure types, especially the pyrochlores, perovskites, and perovskite-related phases (1). Two new lanthanum ruthenate structure types will be described in this article. These are the first examples of isolated ruthenium–oxygen octahedra known for the La–Ru–O system. The structures of $La_7Ru_3O_{18}$ and $La_{4.87}Ru_2O_{12}$ are closely related, even though the first crystallizes in the rhombohedral space group $R\bar{3}c$ and the second crystallizes in the low-symmetry monoclinic space group $P2_1/c$. Both structures can be viewed as cation-deficient versions of the rhombohedral $Sr_5Re_2O_{12}$ structure type (2). Electron counting gives a formal valence of Ru^{5+} in $La_7Ru_3O_{18}$ and $Ru^{4.70+}$ in $La_{4.87}Ru_2O_{12}$, both of which are relatively high oxidation states for ternary oxides of ruthenium.

Many ruthenates have good conduction properties and interesting magnetic behavior (1). Although the occurrence of isolated metal octahedra makes $La_7Ru_3O_{18}$ and $La_{4.87}Ru_2O_{12}$ poor conductors, there is still a possibility for interesting magnetic interactions. Structures with a threefold rotation axis and antiferromagnetic interactions between spins are good candidates for geometric frustration due to the impossibility of satisfying the preferred antiparallel spin arrangement within a triangle of spins (3). This report will present the structures of these two new compounds and will present magnetic data showing that geometric frustration can indeed be found.

EXPERIMENTAL

$La_7Ru_3O_{18}$ and $La_{4.87}Ru_2O_{12}$ were synthesized in bulk quantities using conventional solid state synthesis techniques. Starting materials were La_2O_3, 99.99% (Alfa), and RuO_2, 99.9% (Cerac). To assure accurate weighing of the reagents, RuO_2 was dried at 700°C for at least 1 h and La_2O_3 was dried at 900°C overnight. $La_7Ru_3O_{18}$ was synthesized by mixing the reagents to give a 5:2 molar ratio of lanthanum to ruthenium. Samples were heated at 800 and 875°C for at least 2 days at each temperature. The samples were then annealed at 900°C with multiple grindings until the reaction was complete. The progress of the reaction was followed by monitoring the impurity peak at $d = 3.07$ Å from unreacted La_2O_3, which gradually disappeared from

[1]To whom correspondence should be addressed. E-mail: kpete@princeton.edu. Fax: (609) 258-6746.

0022-4596/00 $35.00

the X-ray diffraction (XRD) patterns after annealing. The synthesis of $La_{4.87}Ru_2O_{12}$ was accomplished by mixing the reagents in a 4.85:2 La:Ru molar ratio, grinding, and then heating for 12 h at 1050°C. Further annealing at this temperature did not change the phase purity.

Single crystals of $La_{4.87}Ru_2O_{12}$ were grown in a KCl flux. Crystals were obtained using a 1:1 molar ratio of La:Ru. 0.5 g of starting material was ground with 5 g of KCl and placed in a 10-ml high form crucible of dense alumina. The mixture was covered with a second crucible of the same size and placed in a small box furnace held at 1000°C for 1–3 days. The furnace was turned off and allowed to cool to <600°C before samples were removed. After the samples were briefly washed with water in a sonic bath, some small pencil-shaped rectangular prismatic crystals of $La_{4.87}Ru_2O_{12}$ were isolated. The majority of crystals were those of $La_3Ru_3O_{11}$, a ruthenate of known structure (4, 5).

An Enraf-Nonius diffractometer was used to collect single-crystal diffraction data. The structure of $La_{4.87}Ru_2O_{12}$ was obtained from a single crystal of dimension $0.007 \times 0.022 \times 0.238$ mm^3. Electron diffraction on powders of $La_7Ru_3O_{18}$ was performed using a Philips CM-200 microscope operating at 200 keV. Magnetic susceptibilities were measured in a Quantum Design Magnetic Property Measurement System (MPMS) in the temperature range of 5–350 K.

Structural data for $La_7Ru_3O_{18}$ were collected at the NIST Center for Neutron Research using the BT-1 32-counter high-resolution powder diffractometer. Room temperature data were collected using neutrons of wavelength 1.5402 Å produced by a Cu (311) monochromator. Collimators with horizontal divergences of 15′, 20′, and 7′ of arc full width at half maximum were used before and after the monochromator and after the samples, respectively. Intensities were measured in steps of 0.05° in the 2θ range 3–168°, and the lattice parameters were determined using GSAS (6). The neutron scattering amplitudes used in all calculations were $b(\mathrm{La}) = 0.827$, $b(\mathrm{Ru}) = 0.721$, and $b(\mathrm{O}) = 0.581$ ($\times 10^{-12}$ cm).

RESULTS AND DISCUSSION

Structural Determination

Although XRD patterns of $La_7Ru_3O_{18}$ had well-defined and well-spaced peaks, it was not possible to find the unit cell dimensions using automatic peak indexing software. Electron diffraction (ED) experiments on $La_7Ru_3O_{18}$ indicated that its symmetry was rhombohedral and estimated the unit cell to be $10 \times 10 \times 60$ Å^3. Images of the $[1\bar{1}00]$ zone showed the $-h + k + l = 3n$ extinction rule for rhombohedral symmetry. Based on this information, it was postulated that $La_7Ru_3O_{18}$ was isostructural with $Ca_5Re_2O_{12}$ and $Sr_5Re_2O_{12}$, two other metal oxides with rhomobohedral symmetry, and unit cells of approximately the same size. Using the crystal structures of these two compounds as the starting point for a structural model, it was possible to refine the structure of $La_7Ru_3O_{18}$ in the same space group ($R\bar{3}c$) using neutron powder diffraction data. However, the 6*a* site at $x = 0$, $y = 0$, $z = 0.25$, which is occupied by Sr in $Sr_5Re_2O_{12}$, was found to be empty in $La_7Ru_3O_{18}$. The observed data was well fit by the refined model, as seen in Fig. 1. The refined cell parameters and atomic positions are given in Table 1, while some selected distances and angles are reported in Table 2.

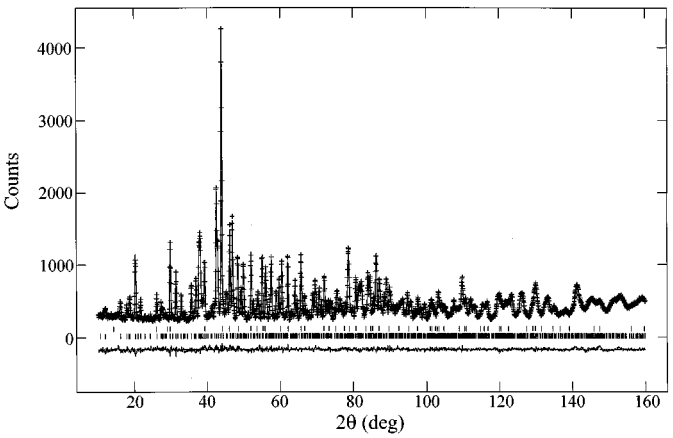

FIG. 1. Observed and calculated powder neutron diffraction pattern for $La_7Ru_3O_{18}$ (97.3 wt%) and La_2O_3 (2.7 wt%) at room temperature. Vertical lines mark the Bragg reflection positions for La_2O_3 (top) and $La_7Ru_3O_{18}$ (bottom). The observed data (crosses) and calculated pattern (solid line) are plotted above the Bragg reflections; their difference plot is shown below.

Due to the availability of single crystals, the structure of $La_{4.87}Ru_2O_{12}$ could be directly determined. The monoclinic cell parameters (spacegroup $P2_1/c$) and atomic positions of this compound are given in Table 3. Relevant distances and angles are listed in Table 4. The unit cell of $La_{4.87}Ru_2O_{12}$ is related to that of $La_7Ru_3O_{18}$ by a factor of $2 \times \sqrt{3} \times 3$, hinting that the symmetry of $La_{4.87}Ru_2O_{12}$ in the *ab* plane may be only slightly distorted from rhombohedral. This is confirmed by views along the *c*-axis of this compound (Fig. 2), which show the same trigonal structural elements as rhombohedral $La_7Ru_3O_{18}$.

Layered View of Structure

When monoclinic $La_{4.87}Ru_2O_{12}$ is viewed perpendicular to the *c*-axis, the layered nature of this compound can be readily discerned (Fig. 3). The layers can be visually grouped into two classes. The thicker layer has three La atoms for every RuO_6 octahedron, while the thinner layer has two La sites per RuO_6 octahedron. The layers alternate, giving this structure the ideal formula of $La_5Ru_2O_{12}$. However,

TABLE 1

Crystallographic data

Formula sum	$La_7\ Ru_3\ O_{18}$
Formula weight	18762.45
Crystal system	Trigonal
Space group	$R\bar{3}c$ (no. 167)
Unit cell dimensions	$a = 9.83677(23)$ Å
	$c = 56.3493(16)$ Å
Cell volume	4721.98 Å^3
Z	12
Density, calculated	6.598 g/cm^3
R_p/R_{wp}	3.19/3.89
χ^2	1.175

Atomic coordinates

Atom	Wyck.	x	y	z
La1	36*f*	0.00948(26)	0.37023(24)	0.187269(35)
La2	36*f*	0.38407(23)	0.05532(22)	0.05085(4)
La3	12*c*	0	0	0.10361(7)
Ru1	18*e*	0.33097(33)	0	0.25
Ru2	12*c*	0	0	0.16169(7)
Ru3	6*b*	0	0	0
O1	36*f*	−0.0051(4)	0.2008(4)	0.22262(5)
O2	36*f*	−0.0034(4)	0.1664(4)	0.01912(6)
O3	36*f*	0.1273(4)	0.1901(4)	0.17895(6)
O4	36*f*	0.1833(4)	0.0587(4)	0.14080(6)
O5	36*f*	0.1847(4)	0.3102(4)	0.10768(6)
O6	36*f*	0.24877(33)	0.10496(31)	0.08287(7)

a partial occupancy of the La2 site results in an actual La:Ru ratio of 1.87:1 in the thinner layer. The thicker layer retains the ideal La:Ru ratio of 3:1. There are a total of four layers in the unit cell of $La_{4.87}Ru_2O_{12}$.

Rhombohedral $La_7Ru_3O_{18}$ shows the same type of layering when viewed perpendicular to its *c*-axis. There are a total of 12 layers per unit cell in this compound. The stacking along the *c*-axis alternates between thicker layers with a 2.67:1 La:Ru ratio and thinner layers with a 2:1 La:Ru ratio. This results in an overall formula of $La_{4.67}Ru_2O_{12}$, which gives the formula $La_7Ru_3O_{18}$ when converted to integer values. It can be seen that one out of every three octahedra in the thick layer is surrounded by only two lanthanum atoms instead of the typical three.

$Sr_5Re_2O_{12}$ has nearly identical layering (2). However, all octahedra in the thick layer are surrounded by three lanthanum atoms. The "extra" large cation in $Sr_5Re_2O_{12}$ resides at midlayer in the thick layer; the rest of the large cations are at either the top or the bottom of the thick layer. This extra cation in $Sr_5Re_2O_{12}$ occupies the Sr4 position. It is in sixfold coordination with oxygen and resides at the exact center of an equilateral trigonal prism. This prismatic site is vacant in $La_7Ru_3O_{18}$. Although La is smaller than Sr, the prismatic site is significantly smaller in $La_7Ru_3O_{18}$ than in $Sr_5Re_2O_{12}$, due to the overall compression of the structure (as seen in the smaller *a* lattice parameter). This is the only major difference between the $La_7Ru_3O_{18}$ and the $Sr_5Re_2O_{12}$ structures. It is interesting to note that, in the thick layer of $La_{4.87}Ru_2O_{12}$, there is no midlayer La site; all three La sites are located at the top or at the bottom of the layer.

Nature of the Layers

In both $La_7Ru_3O_{18}$ and $La_{4.87}Ru_2O_{12}$, the thin layer has Ru atoms sitting in octahedral interstitial sites between two close-packed (CP) layers of formula LaO_3, similar to the CP

TABLE 2

Distances (Å)

Ru1–O1(2×)	1.9891(34)	La1–O4	2.446(4)	La3–O6(3×)	2.4275(34)
Ru1–O5(2×)	1.950(4)	La1–O4	3.1400(35)		
Ru1–O6(2×)	1.9641(26)	La1–O5	2.413(4)	Ru1–Ru1(2×)	5.639(4)
				Ru1–Ru1(4×)	5.700(3)
Ru2–O3(3×)	1.9155(35)	La2–O1	2.470(4)	Ru1–Ru2(2×)	5.516(3)
Ru2–O4(3×)	1.982(4)	La2–O1	2.499(4)	Ru1–Ru2(2×)	5.947(4)
		La2–O2	2.613(4)	Ru1–Ru3(2×)	5.734(1)
Ru3–O2(6×)	1.9734(31)	La2–O3	2.530(4)		
		La2–O4	2.496(4)	Ru2–Ru1(3×)	5.516(3)
La1–O1	2.5548(33)	La2–O5	2.505(4)	Ru2–Ru1(3×)	5.947(4)
La1–O2	2.556(4)	La2–O6	2.432(4)	Ru2–Ru2(3×)	5.707(1)
La1–O2	2.751(4)	La2–O6	2.521(4)	Ru2–Ru3(3×)	5.686(0)
La1–O2	2.647(4)				
La1–O3	2.599(4)	La3–O4(2×)	2.634(4)	Ru3–Ru1(6×)	5.734(1)
La1–O3	2.477(4)	La3–O5(3×)	2.6685(30)	Ru3–Ru2(6×)	5.686(0)

Angles (°)

O2–La1–O2	65.20(11)	O3–La1–O3	49.99(8)
O2–La1–O4	68.45(12)	O4–La1–O3	59.63(4)
O3–La1–O2	60.18(11)	O4–La1–O4	57.68(6)

TABLE 3

Crystal data	
Formula sum	$La_{4.87}Ru_2O_{12}$
Formula weight	1088.69
Crystal system	Monoclinic
Space group	$P1\ 21/c1$ (no. 14)
Unit cell dimensions	$a = 5.5798(6)$ Å
	$b = 10.1286(11)$ Å
	$c = 19.010(2)$ Å
	$\beta = 90.815(4)^\circ$
Cell volume	1074.2(2) Å^3
Z	4
Density, calculated	6.731 g/cm^3
Crystal size	$0.007 \times 0.022 \times 0.238$ mm^3
Linear absorption coefficient (mm^{-1})	22.2
Absorption correction	Multiscan
Min, max transmission	0.546, 0.874

Data collection	
Radiation	Mo$K\alpha$ ($\lambda = 0.71073$ Å)
Diffractometer	Enraf-Nonius CAD4
Monochromator	Graphite
Scan type	ω
Scan range	$-7 < h < 7,\ 0 < k < 14,\ 0 < l < 26$
θ range (°)	2.1–30.0

Refinement	
No. of reflections ($I > 0$)	11608
No. of unique reflections ($I > 0$)	3125
No. of unique reflections ($I > 2\sigma(I)$)	2529
No. of refined parameters	173
R_{obs}/R_{all}	0.054/0.070
Residual electron density (max, min)	6.83, −2.80 e/ Å^3

Atomic coordinates

Atom	Wyck.	Occ.	x	y	z
La1	4*e*		−0.24645(12)	−0.07353(8)	0.04938(4)
La2	4*e*	0.87	0.74172(20)	−0.09052(9)	0.46557(5)
La3	4*e*		0.26961(12)	0.02040(8)	0.34188(4)
La4	4*e*		0.20776(13)	0.14405(8)	0.15749(4)
La5	4*e*		0.24475(11)	−0.22193(8)	0.17509(4)
Ru1	4*e*		0.76245(15)	−0.08752(10)	0.25083(5)
Ru2	4*e*		0.25015(15)	−0.24907(10)	0.00688(6)
O1	4*e*		−0.0280(15)	−0.2938(10)	0.0678(5)
O2	4*e*		0.4588(15)	−0.3682(11)	0.0684(6)
O3	4*e*		0.3199(16)	−0.0855(10)	0.0658(5)
O4	4*e*		0.1749(16)	−0.412(1)	−0.0502(5)
O5	4*e*		0.5262(15)	−0.1923(10)	−0.0477(5)
O6	4*e*		0.0233(14)	−0.1382(10)	−0.0484(5)
O7	4e		0.6195(16)	−0.1261(11)	0.3421(6)
O8	4*e*		0.6592(15)	−0.2621(9)	0.2156(6)
O9	4*e*		1.0513(13)	−0.1728(9)	0.2897(5)
O10	4*e*		0.8999(19)	0.0748(11)	0.2849(7)
O11	4*e*		0.4543(14)	−0.0134(10)	0.2189(5)
O12	4*e*		0.9336(15)	−0.0496(10)	0.1640(5)

TABLE 3—*Continued*

Anisotropic displacement parameters (in Å^2)

Atom	U_{11}	U_{22}	U_{33}	U_{12}	U_{13}	U_{23}
La1	0.01123	0.02748	0.02350	−0.00053	−0.00017	−0.00287
La2	0.02392	0.02302	0.02259	−0.00020	−0.00076	−0.00013
La3	0.01671	0.02250	0.01847	−0.00133	−0.00141	0.00114
La4	0.01876	0.02091	0.02693	0.00030	−0.00637	−0.00200
La5	0.01235	0.02077	0.02256	−0.00080	0.00010	−0.00030
Ru1	0.01009	0.02012	0.01743	−0.00045	0.00079	−0.00003
Ru2	0.01037	0.01873	0.02304	0.00021	−0.00010	−0.00078
O1	0.01639	0.02887	0.02323	0.00593	0.00498	0.00191
O2	0.01335	0.04222	0.03136	0.00267	−0.00360	0.00755
O3	0.01920	0.02768	0.02416	−0.00534	−0.00510	0.00080
O4	0.02655	0.02350	0.01953	0.00340	−0.00196	−0.00699
O5	0.01873	0.02697	0.02380	−0.00516	0.00020	−0.00067
O6	0.01295	0.03388	0.01742	−0.00086	0.00023	0.00792
O7	0.01790	0.04420	0.02845	0.00743	0.00769	0.00227
O8	0.01863	0.01338	0.04954	0.00141	−0.00707	−0.01191
O9	0.01019	0.02473	0.01904	0.00331	−0.00315	0.00175
O10	0.03201	0.02831	0.05231	0.00617	−0.01618	−0.01358
O11	0.00820	0.02557	0.02765	0.00253	−0.00206	−0.00190
O12	0.01821	0.02815	0.01577	0.00375	0.00017	0.00647

layers found in the so-called hexagonal perovskite phases such as $BaRuO_3$ (7) and $BaNiO_3$ (8). One-fourth of the oxygen sites in a close-packed oxygen layer are replaced by the large alkali earth or rare earth actions and, within the layer, each large cation is surrounded by a hexagon of oxygen atoms, giving rise to the AO_3 stoichiometry. One-fourth of the octahedral sites between adjacent AO_3 layers of this type are filled by transition metals. The transition metals are bonded to a triangle of oxygens in each layer, which forces the resulting RuO_6 octahedra to lie flat in the close-packed planes.

The CP layers in both of our compounds are not as regular as those in the hexagonal perovskites. The six oxygens surrounding each La are arranged in irregular hexagons. O–La–O bond angles range from 50° to 68° in $La_7Ru_3O_{18}$ and from 53° to 63° in $La_{4.87}Ru_2O_{12}$. Further distortion comes from displacement of the oxygen atoms, which are found out of the plane of the layer. The spread in the z-coordinate of the oxygen atoms in the LaO_3 layer of $La_7Ru_3O_{18}$ (0.77 Å) is double that of $La_{4.87}Ru_2O_{12}$ (0.38 Å). These are both in contrast to 4H-$BaRuO_3$ and $BaNiO_3$ where all the oxygen atoms in each close-packed plane have exactly the same z-coordinate. It is not surprising that the lanthanum ruthenate structures do not have ideal CP layers since La is significantly smaller than the oxygen it is replacing in the CP layer. The partial vacancy in the La2 site of $La_{4.87}Ru_2O_{12}$ may allow a more regular packing of the CP layer than the one found in the fully occupied CP layer of $La_7Ru_3O_{18}$.

In both compounds, the non-close-packed (NCP) layers differ from the CP layers in the orientation of their RuO_6

TABLE 4

Distances (Å)

Ru1–O7	1.958(10)	La2–O4	3.173(9)	La5–O11	2.549(9)
Ru1–O8	1.974(9)	La2–O5	2.518(10)	La5–O12	2.469(9)
Ru1–O9	1.963(8)	La2–O6	3.178(10)		
Ru1–O10	1.922(11)	La2–O7	2.462(11)	Ru1–Ru1	5.580(1)
Ru1–O11	1.964(8)			Ru1–Ru1	5.580(1)
Ru1–O12	1.956(9)	La3–O1	2.893(10)	Ru1–Ru1	5.716(1)
		La3–O2	2.530(10)	Ru1–Ru1	5.716(1)
Ru2–O1	2.001(9)	La3–O4	2.392(9)	Ru1–Ru1	5.850(1)
Ru2–O2	2.035(10)	La3–O7	2.452(10)	Ru1–Ru1	5.850(1)
Ru2–O3	2.034(10)	La3–O8	2.494(9)	Ru1–Ru2	5.652(2)
Ru2–O4	2.016(9)	La3–O9	2.503(9)	Ru1–Ru2	5.655(1)
Ru2–O5	1.956(9)	La3–O10	2.381(10)	Ru1–Ru2	5.743(1)
Ru2–O6	1.982(9)	La3–O11	2.591(10)	Ru1–Ru2	5.784(1)
				Ru1–Ru2	5.916(2)
La1–O1	2.564(10)	La4–O3	2.978(10)	Ru1–Ru2	5.968(1)
La1–O3	2.447(9)	La4–O5	2.623(9)		
La1–O3	2.744(10)	La4–O6	2.427(9)	Ru2–Ru1	5.652(2)
La1–O3	3.112(10)	La4–O7	2.520(11)	Ru2–Ru1	5.655(1)
La1–O5	2.530(9)	La4–O8	2.689(11)	Ru2–Ru1	5.743(1)
La1–O5	3.174(9)	La4–O9	2.565(9)	Ru2–Ru1	5.784(1)
La1–O6	2.480(10)	La4–O11	2.399(9)	Ru2–Ru1	5.916(2)
La1–O6	2.495(9)	La4–O12	2.492(10)	Ru2–Ru1	5.968(1)
La1–O12	2.399(9)			Ru2–Ru2	5.580(1)
		La5–O1	2.630(9)	Ru2–Ru2	5.580(1)
La2–O1	2.594(10)	La2–O2	2.565(11)	Ru2–Ru2	5.770(2)
La5–O2	2.793(11)	La5–O3	2.535(10)	Ru2–Ru2	5.772(2)
La2–O2	2.592(11)	La5–O8	2.460(8)	Ru2–Ru2	5.803(2)
La2–O4	2.440(9)	La5–O9	2.495(10)	Ru2–Ru2	5.805(2)
La2–O4	2.460(10)	La5–O10	2.343(11)		

Angles (°)

O1–La1–O3	58.8(3)	O1–La2–O4	60.6(3)
O2–La1–O1	57.0(3)	O2–La2–O1	53.1(3)
O3–La1–O2	57.8(3)	O4–La2–O2	62.8(3)
O3–La1–O6	62.2(2)	O4–La2–O6	60.5(3)
O5–La1–O3	63.1(3)	O5–La2–O4	61.6(3)
O6–La1–O5	60.2(3)	O6–La2–O5	58.2(3)

octahedra. The greater thickness of the NCP layers is reflected in the more vertical orientation of the RuO_6 octahedra. The octahedra in $La_7Ru_3O_{18}$ have an edge in the *ab* plane, while the RuO_6 octahedra in $La_{4.87}Ru_2O_{12}$ sit on a single vertex. These are both in contrast to the octahedra in the CP layers, which have one face in the *ab* plane and, as a result, a thin layer profile.

Coordination Polyhedra and Superpolyhedra

The structures of both $La_7Ru_3O_{18}$ and $La_{4.87}Ru_2O_{12}$ contain isolated RuO_6 octahedra. Because superexchange interactions require M–O–M overlap, these compounds can be considered zero-dimensional (0D) in their connectivity. All oxygens atoms in both compounds are part of RuO_6 octahedra. In $La_{4.87}Ru_2O_{12}$, the average Ru–O bond lengths are 1.96 Å for Ru1 and 2.00 Å for Ru2, indicating that Ru may be present in two different oxidation states. In $La_7Ru_3O_{18}$, the average Ru–O bond distances are 1.95, 1.97, and 1.97 Å for Ru1, Ru2, and Ru3, respectively, suggesting that the three Ru sites have the same oxidation state.

Bond valence sum calculations were performed using the method of Brown and Altermatt (9) to quantitatively analyze oxidation states for the different Ru sites. Dussarrat et al. (10) have recently determined the bond valence parameter for Ru^{5+} to be 1.888 Å, a value significantly larger than the bond valence parameter for Ru^{4+} of 1.834 Å deduced by Brese and O'Keefe (11). Since the oxidation states of Ru in $La_7Ru_3O_{18}$ and $La_{4.87}Ru_2O_{12}$ are close to $5+$, the former value was used in the valence calculations.

In $La_{4.87}Ru_2O_{12}$, the Ru1 site in the thick layer is found to have a valence of 5.00 while the Ru2 site in the thin layer has a valence of 4.40. It appears that the additional lanthanum cations in the thick layer help stabilize the higher oxidation state of the Ru1 site. The calculated average valence of Ru in the structure is 4.70, exactly matching the value obtained from the stoichiometry of this compound. This analysis suggests that experimental methods such as XANES used to determine oxidation states (12) may be able to resolve separate peaks for the two different Ru sites.

For $La_7Ru_3O_{18}$, the calculated valences of the Ru1, Ru2, and Ru3 sites are 4.84, 5.11, and 4.76, respectively. The average oxidation state is 4.92, close to the value of 5.00 expected from its stoichiometry. Given the nearly identical oxidation states of the three Ru sites in $La_7Ru_3O_{18}$, the small variations in oxidation state from $5+$ are expected to be chemically insignificant.

A bond valence sum analysis of the unoccupied six-coordinate prismatic site of $La_7Ru_3O_{18}$ suggests a reason for its vacancy. A valence of 2.30 is found using the La–O bond valence parameter of 2.172 determined by Brese and O'Keefe (11). Perhaps the six oxygen anions surrounding this site provide insufficient charge to stabilize the favored $3+$ lanthanum oxidation state.

The upper limit for a La–O bond length was taken to be 3.2 Å. Unlike the Ru atoms, the La atoms in these structures do not have regular coordination polyhedra. However, when the RuO_6 polyhedra of the O atoms in the coordination sphere of each La are drawn, it can be seen that every La atom in both structures is contained within a tetrahedron or octahedron of RuO_6 octahedra. Figure 4 shows these superpolyhedra (*i.e.*, polyhedra of polyhedra) for the three La sites in $La_7Ru_3O_{18}$ and the five La sites in $La_{4.87}Ru_2O_{12}$. The La1 site in $La_7Ru_3O_{18}$ and the La1 and La2 sites in $La_{4.87}Ru_2O_{12}$ are closely related; both are part of the LaO_3 CP layers. Similarly, the La2 site in $La_7Ru_3O_{18}$ and the La3 and La4 sites in $La_{4.87}Ru_2O_{12}$ are related, as are the La3 site in $La_7Ru_3O_{18}$ and the La5 site in $La_{4.87}Ru_2O_{12}$. Although the coordination numbers of

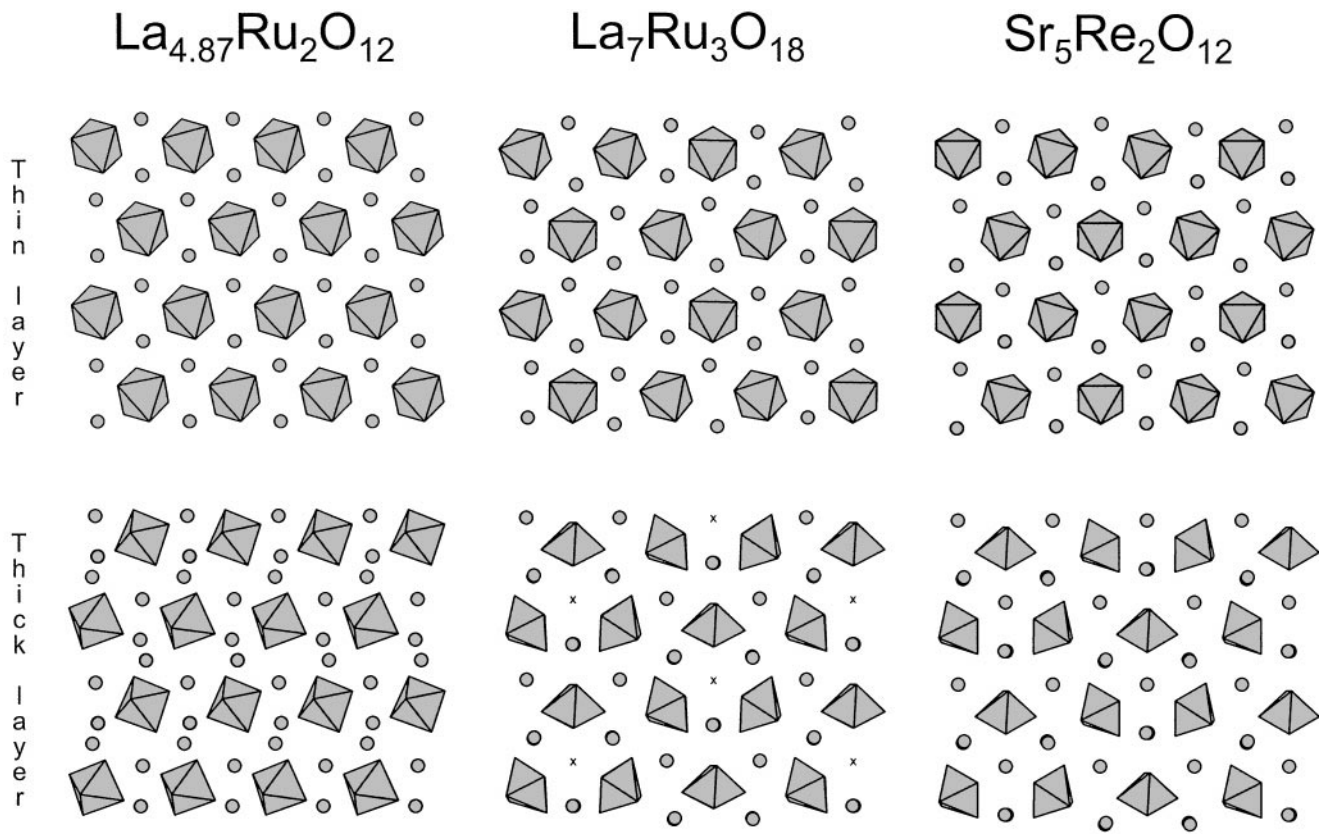

FIG. 2. View parallel to the *c*-axis of $La_{4.85}Ru_2O_{12}$, $La_7Ru_3O_{18}$, and $Sr_5Re_2O_{12}$. Nearly perfect hexagonal arrays of RuO_6 octahedra and La atoms (gray circles) occur. The vacant trigonal prismatic sites in $La_7Ru_3O_{18}$ are marked with an X.

related La sites change between the two structures, related La sites have the same type of superpolyhedra.

The organization of Ru atoms within the structure exhibits further hierarchical arrangement. Each Ru atoms has 12 nearest-neighbor Ru atoms, in a nearly ideal icosahedral arrangement. The nearest-neighbor Ru–Ru distances fall in a relatively narrow range of 5.58 to 5.96 Å in $La_{4.87}Ru_2O_{12}$, and a range of 5.52 to 5.94 in $La_7Ru_3O_{18}$.

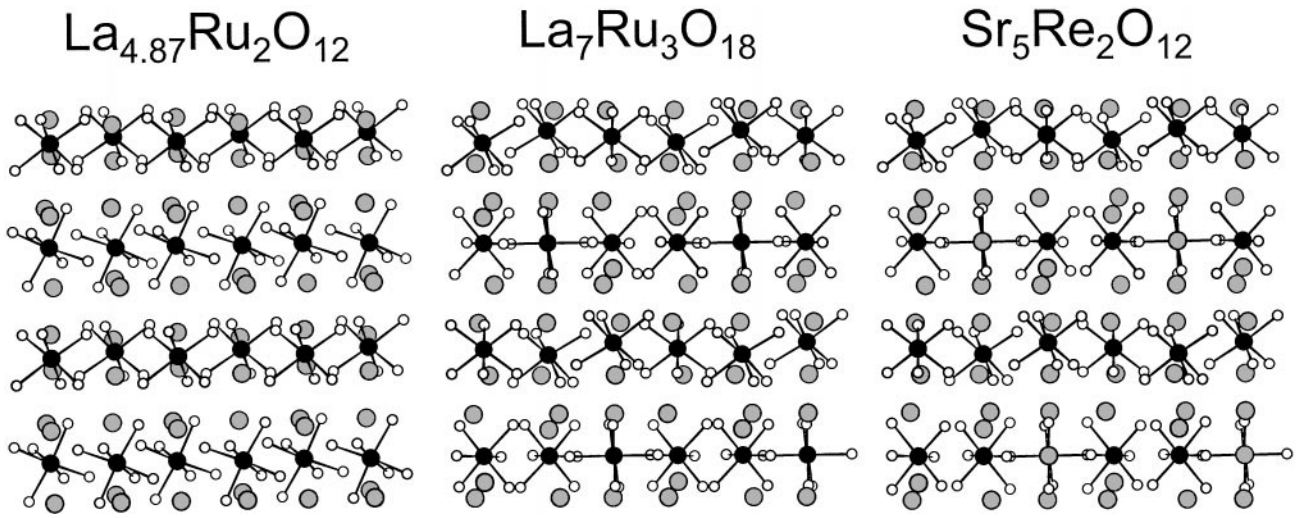

FIG. 3. View perpendicular to the *c*-axis of $La_{4.85}Ru_2O_{12}$, $La_7Ru_3O_{18}$, and $Sr_5Re_2O_{12}$. Small white circles denote O atoms, medium black circles are Ru atoms, and large gray circles are La atoms.

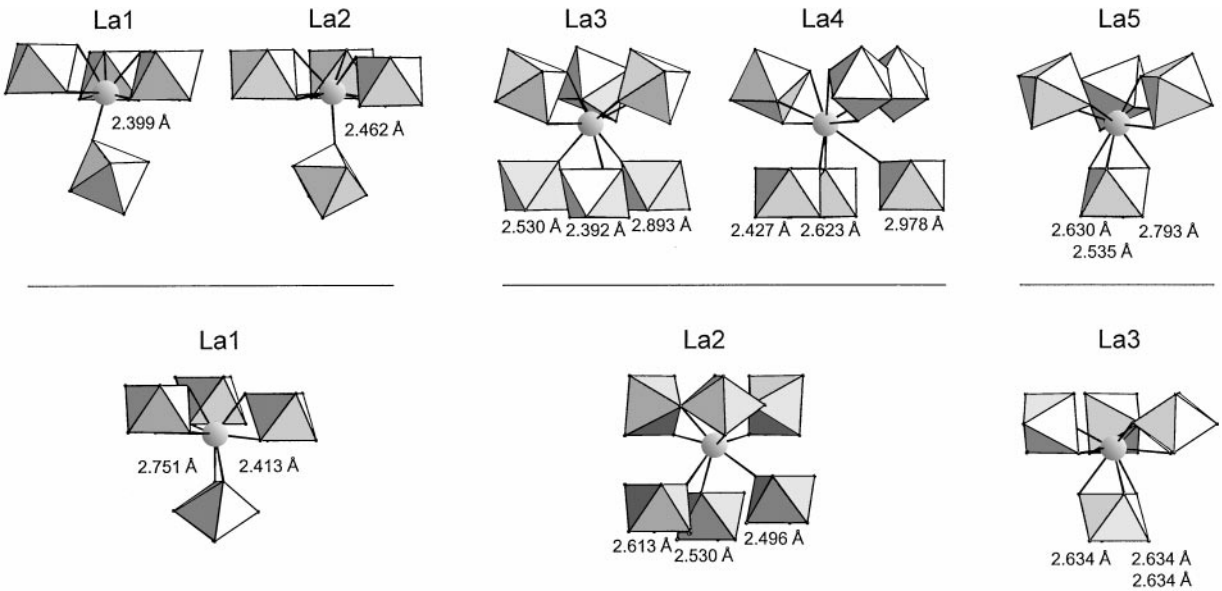

FIG. 4. Coordination superpolyhedra of the La sites in $La_{4.85}Ru_2O_{12}$ (above) and $La_7Ru_3O_{18}$ (below). The three horizontal lines separate the three sets of structurally related positions.

For the latter compound, the distribution of distances falls to 5.64 to 5.71 Å when only the Ru–Ru distances within the *ab* planes are considered. Even though the Ru atoms are well beyond the range of direct orbital interaction, they form a close-packed network, as seen in Fig. 5. The *c*-axis stacking sequence of the close-packed layers in both compounds can be denoted *hc*, with *h* and *c* representing hexagonal or cubic close-packed segments. However, it can be seen that the superpolyhedra of $La_{4.87}Ru_2O_{12}$ are more regular than those of $La_7Ru_3O_{18}$. Both hexagonal and cubic close-packed networks result in atoms being arranged in tetrahedra. Antiferromagnetic coupling between spins within a tetrahedron leads to geometric frustration, as do antiferromagnetic interactions in planar equilateral triangles. It is of interest to determine whether the geometric frustration in these systems (described below) is due to 2D interactions (via triangles) or 3D interactions (tetrahedra). The layered nature of these structures suggests that interactions will be dominantly 2D, while the nearly equivalent Ru–Ru distances and the close-packed arrangement of Ru atoms suggests that the 3D picture may be more relevant.

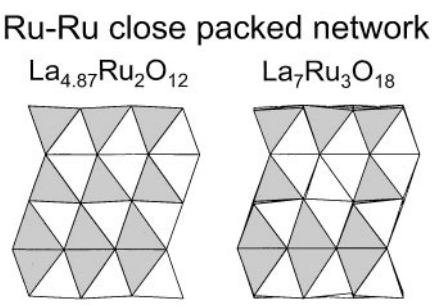

FIG. 5. Close-packed network of Ru atoms in $La_{4.85}Ru_2O_{12}$ and $La_7Ru_3O_{18}$ demonstrating the *hc* stacking sequence of layers.

Physical Properties

$La_{4.87}Ru_2O_{12}$ and $La_7Ru_3O_{18}$ are both electrically insulating. Powders of $La_{4.87}Ru_2O_{12}$ are a dull black color, while those of $La_7Ru_3O_{18}$ are brown. Two probe resistance measurements on pressed powder pellets gave $R = 100\ \text{k}\Omega$ for $La_{4.87}Ru_2O_{12}$ and $R > 2\ \text{M}\Omega$ for $La_7Ru_3O_{18}$. Due to the high resistivities of these compounds, more detailed measurements were not performed.

Magnetic data for both compounds were collected using an applied field of 0.1 T. Field-cooled (FC) and zero-field-cooled (ZFC) data were found to be identical. A plot of the FC magnetic susceptibility vs temperature is shown in Fig. 6. $La_7Ru_3O_{18}$ was found to order at 14 K with a 0.1 T applied field. Under a 0.1 T field, $La_{4.87}Ru_2O_{12}$ did not order in the measured temperature range.

Inverse susceptibility plots for $La_7Ru_3O_{18}$ and $La_{4.87}Ru_2O_{12}$ are presented in Fig. 7. Linear fits to the high-temperature data show that both compounds have similar Curie–Weiss temperatures ($\theta = -58$ K for $La_7Ru_3O_{18}$ and $\theta = -85$ K for $La_{4.87}Ru_2O_{12}$), indicating the presence of medium-strength antiferromagnetic interactions between the Ru spins. We find an effective moment of 3.49 μ_B for $La_7Ru_3O_{18}$, a value smaller than the ideal moment of 3.87 μ_B expected for Ru^{5+}. The effective moment of $La_{4.87}$

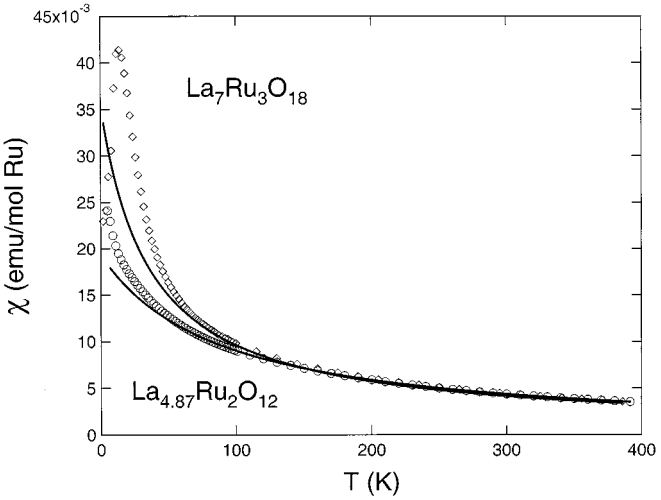

FIG. 6. Temperature dependence of magnetic susceptibility measured at 0.1 T for $La_7Ru_3O_{18}$ (diamonds) and $La_{4.85}Ru_2O_{12}$ (circles). Curie–Weiss fits to high-temperature data are shown as solid lines.

Ru_2O_{12} is 3.64 μ_B, close to the expected moment of $Ru^{4.70+}$.

In the absence of complicating factors, the AFM ordering temperature is expected to be on the order of the Curie–Weiss temperature, θ. It is apparent from plots of the temperature dependence of the susceptibility (Fig. 6) and inverse susceptibility (Fig. 7) that the ordering is frustrated in both compounds. At a field of 0.1 T, $La_7Ru_3O_{18}$ does not order until it is cooled to 14 K. An even more extreme suppression occurs in $La_{4.87}Ru_2O_{12}$, which does not order at all in measurements down to 5 K. The frustration index (3) ($f = -\theta/T_c$) for the 5 T data on these two compounds is $f = 4$ for $La_7Ru_3O_{18}$ and $f > 17$ for $La_{4.87}Ru_2O_{12}$.

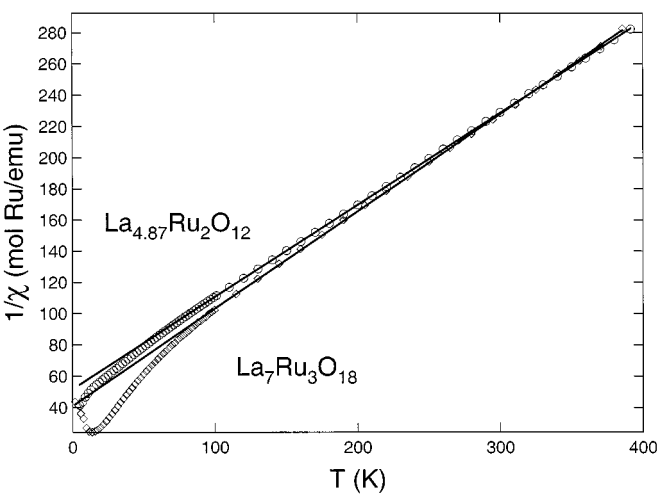

FIG. 7. Temperature dependence of the reciprocal susceptibility measured at 0.1 T for $La_7Ru_3O_{18}$ (diamonds) and $La_{4.85}Ru_2O_{12}$ (circles). Curie–Weiss fits to high-temperature data are shown as solid lines.

An interesting feature of the susceptibility data for both compounds is the enhanced magnetism (relative to the values expected from the Curie–Weiss law) at low temperatures, which seems to be in contrast to the antiferromagnetic exchange constants determined from the Curie–Weiss fits. This behavior has been observed in other geometrically frustrated compounds (13). The increase in magnetism is attributed to a decrease in the interaction strength between spins that occurs as the distance between active spins increases through the formation of spin clusters.

Two factors that commonly lead to frustration of magnetic ordering are structural disorder and certain lattice geometries. To show that a compound is geometrically frustrated, it is necessary to show that structural disorder is not playing a role in the lowering of the ordering temperature. The structure of $La_7Ru_3O_{18}$ is fully ordered, and all Ru positions within a layer are equivalent. There is a possibility for disorder effects in $La_{4.87}Ru_2O_{12}$, due to the partially occupied La site. Although structural disorder can keep compounds from magnetically ordering, it will not prevent short-range order from occurring. In the inverse susceptibility plot of Fig. 7, it can be seen that $La_{4.87}$ Ru_2O_{12} is only small deviations from linearity, even at temperatures well below θ, indicating that almost no short-range order is present.

It is interesting to compare $La_{4.87}Ru_2O_{12}$ to the magnetoplumbite structure, another magnetically frustrated compound, $SrGa_4Cr_8O_{19}$. This chromium-containing compound is one of the most strongly frustrated systems known. The magnetic Cr(12*k*) site is 86% occupied (14), indicating that there is similar structural disorder in hexagonal $SrGa_4$ Cr_8O_{19} and monoclinic $La_{4.87}Ru_2O_{12}$. Since the disorder in $La_{4.87}Ru_2O_{12}$ occurs at the nonmagnetic La site, it is expected that disorder will play a smaller role $La_{4.87}Ru_2O_{12}$ than in the magnetoplumbite structure, which is known to be geometrically frustrated. For these reasons, the geometrical arrangement of spins in $La_{4.87}Ru_2O_{12}$ is believed to be the major factor responsible for the observed magnetic frustration. Using the classification scheme of Ramirez *et al.* (3), we can state that $La_{4.87}Ru_2O_{12}$ is a new member of the class of strongly geometrically frustrated (SGF) antiferromagnets since it has a frustration index of $f > 10$.

CONCLUSIONS

The similar Curie–Weiss θ values for $La_7Ru_3O_{18}$ and $La_{4.87}Ru_2O_{12}$ indicate that similar strength magnetic interactions occur in these two structurally related phases. Magnetic measurements demonstrate that the geometry of these compounds affects their magnetic properties, as both have frustrated magnetic ordering. The origin of the geometric

frustration is either the threefold (or pseudo-three-fold) rotation axis in the *ab* plane or the tetrahedral network of Ru–Ru interactions that occur due to the close-packed patterning of Ru atoms. It is impossible to decide between the 2D or 3D scenarios based on only the structural information.

Monoclinic $La_{4.87}Ru_2O_{12}$ can be counted among a short list of strongly geometrically frustrated antiferromagnets, despite the fact most other SGF compounds have a higher degree of symmetry. Even though a true threefold rotational symmetry is present in the *ab* plane of rhombohedral $La_7Ru_3O_{18}$, this compound is less frustrated than $La_{4.87}Ru_2O_{12}$, probably due to the greater offsets of the RuO_6 octahedra along the *c*-axis. Valence bond calculations suggest that ruthenium is present in two different oxidation states (5.0 and 4.4) in the two different layers of $La_{4.87}Ru_2O_{12}$. Perhaps this results in decreased interactions between layers and therefore a network of spins that is more two-dimensional in character. Recent experiments on chromium ferrites with the same Kagomé arrangements of spins as $SrGa_4Cr_8O_{19}$ but with larger *c*-axis separations between the magnetic layers show greatly enhanced magnetic frustration (15), showing that dimensionality can indeed have an important role in determining the degree of frustration of a material. Further measurements are necessary to resolve the true dimensionality of $La_{4.87}Ru_2O_{12}$ and $La_7Ru_3O_{18}$.

ACKNOWLEDGMENTS

This work was supported by the National Science Foundation Grant No. DMR-9725979. P. K. gratefully acknowledges support from a National Science Foundation Graduate Fellowship.

REFERENCES

1. P. Khalifah, R. W. Erwin, J. W. Lynn, Q. Huang, B. Batlogg, and R. J. Cava, *Phys. Rev. B* **60,** 9573 (1999), and references contained therein.
2. H. A. Mons, M. Schriewer, and W. Jeitschko, *J. Solid State Chem.* **99,** 149 (1992).
3. A. P. Ramirez, *Annu. Rev. Mater. Sci.* **24,** 453 (1994).
4. F. A. Cotton and C. E. Rice, *J. Solid State Chem.* **25,** 137 (1978).
5. F. Abraham, J. Trehoux, and D. Thomas, *Mater. Res. Bull.* **12,** 43 (1997).
6. A. C. Larson and R. B. Von Dreele, "General Structure Analysis System," Report no. LAUR086-748. Los Alamos National Laboratory, Los Alamos, NM.
7. S.-T. Hong and A. W. Sleight, *J. Solid State Chem.* **128,** 251 (1997).
8. Y. Takeda, F. Kanamaru, M. Shimada, and M. Koizumi, *Acta Crystallogr. B* **32,** 2464 (1976).
9. I. D. Brown and D. Altermatt, *Acta Crystallogr. B* **41,** 244 (1985).
10. C. Dussarrat, F. Grasset, R. Bontchev, and J. Darriet, *J. Alloys Compd.* **233,** 15 (1996).
11. N. E. Brese and M. O'Keefe, *Acta Crystallogr. B* **47,** 192 (1991).
12. S. Ebbinghaus, Z. Hu, and A. Reller, *J. Solid State Chem.*, in press.
13. P. Schiffer and I. Daruka, *Phys. Rev. B* **56,** 13712 (1997).
14. A. P. Ramirez, G. P. Espinosa, and A. S. Cooper, *Phys. Rev. Lett.* **64,** 2070 (1990).
15. I. S. Hagemann, A. P. Ramirez, Q. Huang, and R. J. Cava, to be published.